Chapter I
Introduction

Introduction

Processes involving the chemical transformation of solids play an increasingly important role in modern technology as sophisticated and costly solids can be produced by reaction of cheap precursory solids. To obtain the desired purity, structure and texture of the material, a control of reaction is necessary.[1]

There is often an intimate relationship between the physical properties of a solid and its chemical composition or chemical processes within it. In particular, many properties depend upon deviation from the ideal structure and to understand and control them, we must turn to the chemistry of the solids.

Differential thermal analysis-thermogravimetry (DTA-TG) techniques plays an increasingly important role in the determination and identification of materials, change in phases, crystalline structure, inversions, melting reactions, thermal decomposition, solid state reactions, quantitative analysis and kinetic studies [2]. Knowledge of various energetic and structural changes taking place in solid heterogeneous substances during thermal treatment is greatly facilated through the aid of differential thermal analysis. Thermogravimetry is the science of weighing substances while they are being heated. The major of the thermal decomposition studies were carried out on solids which upon decomposition a gas is evolved and a solid residue is remained, the composition of solid residue is in general known. The thermal analysis data indicate the temperature at which theoretical weight loss is

achieved and this is arbitrarily selected as the minimum temperature for calcination. The actual calcination temperature employed may be higher, but for convenience the temperature was kept below the onset of sintering. The selection of calcination time, temperature and atmosphere would be expected to influence the particle size and reactivity of the resulting material [3].

One of the interesting applications of thermal analysis is the investigation of the behaviour and kinetics of solid state reactions. Kinetic measurements are perhaps most frequently undertaken to obtain information concerning the mechanism of a specified reaction. Such investigations may include characterization of reaction stoichiometry, particularly product compositions where mixtures are formed and the identification of intermediates. This information can be of value in contributing towards the theoretical development of the subject generally, by identifying the factors that control reactivity and understanding the significance of participating steps. Empirical measurements of reaction rates may also be of value in the development of industrial processes where the principal objective may be to establish the most effective and efficient condition that can be exploited in production so that costs, waste and pollution are minimized [4]. In many cases, the kinetics of the thermal decomposition reactions were followed, depending on system investigated, by measurement the pressure of gas released in a closed volume as a function of time and by analysis of products by mass spectroscopy. However, more recently (DTA-TG)

analytical techniques are more widely used, since they provide a rapid and convenient method for the quantitative investigation of decomposition reaction [5]. Microscopic observations were also made in few cases [6]. The kinetic of solid state thermal decomposition reactions can be followed either by isothermal or non-isothermal (dynamic) methods. The time required for an adequate series of isothermal experiments is a considerable disadvantage, and especially when the amount of the reactants available is also limited, therefore it becomes most desirable to obtain maximum information from a single kinetic experiment. Much attention has also been directed at the use of non-isothermal method to follow the kinetics of solid-state reactions [7].

The purpose of many kinetic studies is to obtain information concerning the reaction mechanism [8]. Most solid state decompositions are governed by the movement of the reaction interface and hence, the kinetics [9]. The kinetics of the thermal decomposition of solid-state materials is highly complex and frequently controversial subject. This kinetic is affected by experimental factors [2,10], such as a heating rate, a particle size, sample mass and holder design. Two further important factors are the effect of enthalpy of reactions upon sample temperature and atmosphere. Moreover the use of different methods of kinetic analysis of both isothermal and non-isothermal thermogravimetric data obtained on one system to find activation energy and other kinetic parameters usually gives different results. Criteria for the excellence of kinetic fits reported in research publications aren't always specified and,

in practice, identification of the preferred rate equation may be a personal decision between the research workers concerned based on undisclosed reasons [4].

X-ray diffraction furnishes a rapid and an accurate method for the identification of crystal structure of various solid compounds and identification of the actual compound from its structure [11]. It can also determine the arrangement of molecules in crystal, phase identification, quantitative analysis of a mixture of phases, particle size analysis, characterization of physical imperfections and in situ studies of reactions. Comparing diffraction patterns from crystals of known composition with patterns from crystals of unknown compounds permits the identification of unknown crystalline compounds.

The electrical conductivity in solids [11] is very important property to differentiate between various types of solids. The electrical conductivity of oxide materials encompasses a wide range of values, which characterize insulator, semiconductors and metallic materials. There are many theories and mechanisms to explain the electronic conduction in solids. According to band theory if the valence bands, which contain electrons, are completely filled while the conduction bands are empty, the material is considered as insulator and shows a very poor conduction. If, on the other hand, the highest-lying occupied band contains large fractions of both occupied and empty states, the solid is a metal and shows a good conduction. Finally, if this highest occupied band contains only small concentration of occupied or empty states, the

material is a semiconductor and shows an intermediate conductivity. There is, however, another difference in the electrical properties of these three materials. The most important of these is the effect of temperature on the electrical conductivity. As a general rule the electrical conductivity of metals decreases with increasing its temperature, while the conductivity of semiconductor and insulators show a reverse temperature effect with the respect to the nature and behaviour of charge carries in these materials. In general the conductivity (σ) is given by [11]: $\sigma = n\ e\ \mu$,where n is the number of current carrying species, e is their charge and μ their mobility.

In metals, electrons are the main charge carriers and move throughout freely; they aren't localized or bound to atomic sites. There is therefore essentially no activation energy required for the conduction process. The number of mobile electrons is large and essentially constant, but their mobility gradually decreases with rising temperature due to electron-phonon collisions. Consequently, conductivity gradually drops with rising temperature. In semiconductors, the number of mobile electrons is usually small. This number may be increased in one of two ways, either by rising the temperature so as to promote more electrons from the valence band to the conduction band, or by doping with impurities that provide either electrons or holes. In the first of these, n and therefore, σ, rise exponentially with temperature (Intrinsic semiconductivity), the relatively small change in μ with temperature are completely swamped by the much large changes in n. In the second of

these, extra mobile carriers are generated by the addition of dopants at low temperature (Extrinsic conductivity). The concentration of these extra mobile carriers is much greater than the thermally generated intrinsic carrier concentration. Consequently concentration is independent of temperature and σ shows a slight decrease with temperature due to mobility effect mentioned above. In insulators, however, electrons are not free to move throughout the bulk of materials but are bound to atomic sites. They differ from semiconductors only in the magnitude of their conductivity, which are usually several orders of magnitude lower. Thus, the conductivity of insulators is also sensitive to both temperature and dopants.

Semiconductor with only few electrons in the highest occupied doped level called n-type and those with only few empties, or holes, are called p-type.

Inorganic solids that exhibit magnetic effects other than diamagnetism, which is a property of all substances, are characterized by having unpaired electrons on metal cations [11]. Magnetic behaviour is thus restricted mainly to compounds of transition metals and lanthanides, many of them possess unpaired d and f electrons, respectively. Several magnetic effects are possible. The unpaired electrons may be oriented at random on the different atoms, in which case, the material is paramagnetic. They may be aligned so as to be parallel, in which case the material possess an overall magnetic moment and is called ferromagnetic. Alternatively, they may be aligned in antiparallel

fashion, giving zero over all magnetic and antiferromagnetic behaviour. If the alignment of the spins is antiparallel but unequal numbers in the two orientations, net magnetic moment results and the behaviour is ferrimagnetic. Paramagnetic substances are attracted by a magnetic field, whereas, diamagnetic substances experience a slight repulsion. There is a strong and analogies between magnetic properties and corresponding electrical properties such as ferroelectricity. The susceptibility (X) of the different kinds of magnetic materials are distinguished by their different temperature and magnetic field dependence as well as by their absolute magnitude. For all materials the effect of increasing temperature is to increase the thermal energy possessed by ions and electrons. There is, therefore, a natural tendency for increasing structural disorder with increasing temperature. For paramagnetic materials, the thermal energy of ions and electrons acts to partially cancel the ordering effect of the applied magnetic field. Indeed, as soon as the magnetic field is removed the orientation of the electron spins becomes disordered. Hence, for paramagnetic materials X decrease with increasing temperature, in Curie/Curie-Weiss law fashion [11]. For ferro- and antiferromagnetic materials, the effect of temperature is to introduce disorder into the otherwise perfectly ordered parallel/antiparallel arrangement of spins. For ferromagnetic materials, this leads to a rapid decrease in X with increasing temperature. For antiferromagnetic materials, this leads to a decrease in the degree of

antiparallel ordering, an increase in the number of disordered electron spins and hence an increase in X [11].

I-1. Mixed-Valence Compounds:

Chemical compounds consisting of an element (usually a metal) in two different oxidation states are said to exhibit mixed valence. The conductivity of semiconducting transition metal compound is often increased when the transition element is present in more than oxidation state. Such materials are known as controlled valence or mixed valence semiconductors. Mixed-valence chemistry is as old as chemistry itself, some of the well known mixed-valence compounds being prussian blue ($Fe_4[Fe(CN)_6]_3.14H_2O$) and magnetite (Fe_3O_4). Mixed-valence chemistry, however, encompasses a large variety of solids with fascinating properties formed by nearly a third of the elements in the periodic table. Since variable valence is a prerequisite for mixed valence, it is quite common among the compounds of transition metal, Ce, Eu and Tb, as well as some of the post-transition elements with stable ns^2 and ns^0 electronic configuration such as Ga, Sn, Sb, Tl, Pb and Bi. Most mixed valence compounds contains electronegative counterpart anions such as halides, oxide, sulphide or molecular ligands containing electronegative atoms. Mixed valence occurs in minerals (e.g. Fe_3O_4), metal chain compounds, dimers and oligomers and metal complexes, and even in organic and biological systems [12]. Mixed-valence transition metal oxide gels are also well known [13]. Oxides of

transition metal always display effects due to mixed valences because a change of stoictiometry can be accommodated by a change in the occupation number of shell. The delocalization of electrons in excited states is expected to be greater than in the ground state, and therefore the optical spectra of compounds with mixed valences could show new bands which are associated with electron transfer [12]. Many metal oxides are mixed-valence compounds [14], containing a transition element that can not be assigned a unique integral oxidation state. This category includes not only the non-stoichiometric and doped compounds, but also many stoichiometric ones such as Fe_3O_4 and Ti_4O_7. An interesting question is whether one should assign different integral oxidation states to the element concerned (Fe^{2+} and Fe^{3+}, or Ti^{3+} and Ti^{4+}), or rather an equal, but fractional oxidation state (for example $Fe^{2.67+}$ or $Ti^{3.5+}$), such a distinction forms the basis of the classification scheme for mixed valence compounds proposed by Robin and Day [13] based on valence delocalization coefficient; α, the magnitude of which depends on the energy difference between two states; ΔE, and widely used by chemists. Class I. compounds have distinguishable oxidation states in very different environments, so that essentially no electronic phenomena can be associated with charge transfer between them where ΔE is large and α is small, so the insulation occurs. This situation is rather uncommon in transition metal oxides, but an example might be KCr_3O_8, containing octahedral Cr^{3+} and tetrahedral CrO_4^{2-} ions. Class II compounds are ones where different oxidation states can be identified by structure or

electronic studies, but where the energy required for electron transfer is small, so the semiconduction occurs. In class III compounds on the other hand, a metal atom has equal fractional oxidation states and α becomes large, normally associated with metallic conduction. Thus the metallic tungsten bronzes should be assigned to class III, whereas many semiconducting oxides such as $Li_xMn_{1-x}O$ and $Fe_xCo_{3-x}O_4$ fall in class II. The electron localization associated with class II character in doped and non-stoichiometric oxide semiconductors is caused by a combination of the potential field of defects, structural disorder, and lattice interactions forming polarons. Class II behaviour can also be found sometimes in stoichiometric compounds, where it is the lattice interactions essentially the different atomic geometries appropriates to different oxidation states, which cause electronic trapping [14]. The electron hopping between the sites in class I compounds is not favoured since ΔE is large. In class III compounds, on the other hand, the electrons would be delocalized. Hopping conduction [12] can be considered simply as diffusion of carriers through the lattice with the assistance of phonons. At low temperature there are few phonons present, and the hopping probability is small, but at high temperatures there are exponentially more phonons present and the hopping probability is much larger. According to hopping mechanism the electron transfer from one localized state in crystal lattice to adjacent sites, such as the transfer of electron from V^{+4} to V^{+5} in V_2O_5[12].

In order to describe the electron transfer in mixed valence compounds properly, one would have to consider the coupling between the electronic and vibrational motions. Experimentally, the frequency of optical intervalence transition gives an estimate of the energy required for thermally activated electron transfer. The intensity of the optical intervalence transition gives information on α. One of the most characteristic features of mixed-valent class II compounds is the structureless broad intervalence absorption band in the visible and infrared. In certain mixed-valence compounds, the presence of more than one oxidation state can be recognized from formula, while in some others the formula indicates an apparently integral oxidation state although the oxidation state is rather unusual for the element in question [12]. Fe_3O_4 and Ti_4O_7 provide examples of compounds where the chemical formula itself indicates mixed valence. The case of AgO illustrate a different situation, of hidden mixed valence, where a study of the structure and physical properties is necessary to show that different oxidation states are present ($Ag^+ Ag^{3+} O_2$) [14]. Magnetic interactions can also be observed when the two valence states have non zero magnetic moments [16].

Fe_3O_4 consisting of iron in 2+ and 3+ oxidation states has the inverse spinel structure, with all Fe^{2+} ions and half of the Fe^{3+} ions located in octahedral sites in the oxygen network and the remaining half of the Fe^{3+} ions located on tetrahedral sites. It undergoes a ferrimagnetic-paramagnetic transition around 850°K and another

transition around T_V = 123°K (Verwey transition). The material is semiconductor both above and below the Verwey transition [12].

Controlled valence semiconductors find application as thermistors, thermally sensitive resistors. In these, use is made of the large temperature dependence of conductivity, associated with the fact that these materials are hopping semiconductors. For example, the material $Li_{0.05}Ni_{0.95}O$ shows Arrhenius-type conductivity behaviour over a wide temperature range up to 473°K. The activation energy is about 0.15ev. Since the conductivity behaviour is reproducible, lithium nickel oxide can be used in devices to control and measure temperature. In order to achieve reproducibility, materials that are insensitive to impurities must be used, e.g. Fe_3O_4, Mn_2O_3, Co_2O_3 doped NiO and certain spinels [11].

I-2. Literature Survey:

Studies of the thermal analysis and kinetics of the thermal decomposition of metal oxalates have drawn the interest of several investigators [9,16-19], since the thermal decomposition of such materials results in products e.g. oxides or metals, which may possess pores, lattice imperfections and other characteristics; necessary for its function as reactive solids and some oxalates may be considered as economic catalyst precursors [1]. The chemical changes in oxalates are complex than carbonates and hydroxide [20]. The thermal decomposition of oxalates proceeds by several routes. Boldyrev et. al. [16] have suggested that these may be classified according to the three principle reaction:

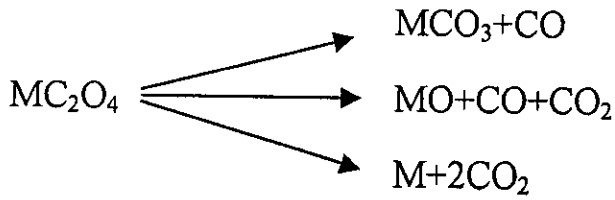

Some oxalates such as calcium oxalate decomposes to a carbonate, other such as zinc oxalate decomposes to an oxide, a further groups of oxalates if decomposed in an inert atmosphere produce the metal as a solid product, but if they decomposed in air the metal oxide is produced. The production of silver metal as a decomposition product of silver oxalate in all atmospheres including, oxygen, nitrogen, air and carbon dioxide is unique [21]. Dollimore et. al. [17], reported the TG analysis of several oxalates in air and nitrogen, where it is shown that in some cases the decomposition proceeds directly to oxide, but that in others the metal is first formed and is subsequently oxidized in air to the oxide. The experiments showed two classes of oxalate decomposition, in the first class, are materials such as oxalates of Cr, Mn, Fe and Zn, which produce oxides as a result of decomposition in air or nitrogen, and in the second class, are oxalates such as those of Co, Ni and Cu which decomposed to produce oxide in air but metal in nitrogen. In general the decomposition in nitrogen is simpler than that in air, produce the metal or the lower oxides.. For metal oxalates [22] the possible decomposition stages were found to include firstly the formation of an anhydrous oxalate which converted to metal oxide in the presence of air. An intermediate carbonate stage for most oxalates wouldn't be expected to

be stable[22]. The presence of oxygen [23,24] affects the decomposition of transition metal oxalates. In oxalates of bivalent metal [25] i.e.:

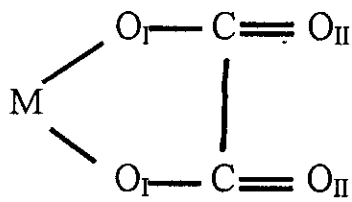

The extent to which the metal-O_I bond is covalent depends on electronegativity of the metal, the decomposition will occur when the temperature is reached at which repture of M-O_I link is possible or at which the C-O_I bond occurs. As the electronegativity of metal ion increases, so the bond strength of the M-O_I bond will increase and according to Fujita et. al. [26], the C-O_I bond will become weaker. For a series of oxalates of divalent transition metal with increasing electronegativity, when the decomposition occurs by repture of the two M-O_I bond to produce the metal with liberation of $2CO_2$, then the decomposition temperature will increase along the series, but if C-O_I bond break first, this would be followed by repture of the second M-O_I bond because the inability of the metal to accommodate two oxygen atoms and this will lead to evolution of an equimolecular amount of CO and CO_2 and the formation of MO with decrease in decomposition temperature along the series [27].

It has been already pointed out that the course of oxalate decomposition may be affected by the environment, ignorance of this lead early workers to claim that oxalate decomposition were exo in character, where it is now quite clear that the majority of such

decomposition in an inert atmosphere are endo [28,29]. The most obvious change caused by the environment is observed when the actual products are different due to influence of the surrounding gas atmosphere. The exo nature of decomposition is usually associated with an interaction of one or more of end products with environmental atmosphere [21]. Cupper oxalate [18] and silver oxalate [28] decomposed in nitrogen with an exo-reaction. These decompositions are often described as autocatalytic. Ammonium oxalate [18] decomposes endothermically in both nitrogen and oxygen. The decomposition remains endo in oxygen because there is no solid product, since all decomposition products are gaseous and there is no surface to act as a catalyst for oxidation reaction. When the decomposition of oxalates leads to the formation of carbonates then its decomposition peak is endo under all environments as can be seen in decomposition of lithium oxalate [30].

There is another environmental effect, namely the shape and size of container crucible and the material with which it was constructed. Thus the endo or exo character of decomposition of magnesium oxalate can be affected. The decarboxylation peak in oxygen is endo except in presence of catalyst [31] (as Mg is a poor catalyst). If a Pt crucible is used this can provide the appropriate catalyst surface and the reaction become exo overall. In particular the variation of mass of sample has a profound effect on the rate-determining step in the kinetic determination of the reaction [32].

The dehydration step in thermal treatment of most oxalates seems to be always endo in character and unaffected by environment except for lithium oxalate [30,33], which doesn't show the endo character for dehydration since it doesn't occur in hydrated form. The TG curves of most transition metal oxalates show no stable dehydration step when obtained at a high heating rate, whereas DTA curves distinguish separate stage. The dehydration process in vacuum or low water vapour pressure often produces an amorphous anhydride material with a high surface area, whilst at higher vapor pressure of water a crystalline anhydride product results with a much smaller surface area. This behaviour is called Smith-Topley effect, it has been observed for dehydration of $MgC_2O_4.2H_2O$ [34]. Wendlandt [35] studied the thermal decomposition of rare earth metal oxalate of Sc, Y, La, Ce, Pr, Nd, Sm, Eu, Gd, Ho and Er and found that the hydrated water come off in the temperature range of 313°K to 333°K. Although the thermal properties of metal oxalates have been extensively studied, few studies have been made of metal oxalate type complexes. Wendlandt and George [36] carried out TG of $K_3[M(OX)_3].3H_2O$ (where M = Cr^{3+}, Fe^{3+} and Co^{3+}) and $K_3[Rh(OX)_3].2.5H_2O$. Tanaka and Nanjo [37] have followed the change in valence state of central metal ions on thermal decomposition of $K_3[M(OX)_3].3H_2O$ (where M = Fe^{3+} and Co^{3+}), they suggested that the decomposition of these complexes is initiated by electron transfer from the coordinates oxalate ion to central metal ion.

A considerable amount of information on the kinetics of thermal dehydration and thermal decomposition of the individual oxalates has been reported [38-42]. Dollimore [43] has discussed the thermodynamic, kinetic and textural features of metal formation of the decomposition of oxysalts.

Dollimore and Evans [21] showed that under vacuum, the decomposition products of silver oxalate are silver metal and carbon dioxide in an autocatalytic reaction. However, the decomposition could be drastically altered by the preparation of sample. They also showed that the silver oxalate decomposed to silver metal in all atmospheres with an exothermic nature. Subsequent investigation into the thermal decomposition of silver oxalate gave markedly different results and consequently different interpretations of kinetic data. The presence of finely divided silver metal as a decomposition product has industrial applications in the catalyst industry, and silver oxalate can be found being used as precursor for silver metal to be used in the production of a catalyst for the attempted epoxidization of ethene to ethylene oxide [44,45]

The thermal decomposition of $CdC_2O_4.3H_2O$ has been studied in air and nitrogen atmospheres by many authors [17,18]. They found that the end product in nitrogen is Cd and in air is CdO.

Dollimore et. al [17] studied the thermal decomposition of ZnC_2O_4 in air and nitrogen and found that the end product in air or nitrogen is ZnO in both atmospheres. Kinetics of the thermal decomposition of zinc oxalate dihydrate have been examined by several workers[38,46].

The thermal decomposition of cupper oxalate differs substantially from that of the other transition metal oxalates [18], where cupper oxalates exhibits a strongly exothermic decomposition reaction when heated in N_2. This reaction is described as autocatalytic. The prevailing atmosphere affects the decomposition routes. Decomposition may be preceded by endothermic dehydration step. In oxygen, the over all reaction is strongly exothermic, owing to the reaction of evolved CO with O_2 to form CO_2 and the oxidation of metal decomposition product to a metal oxide. Gleizes et. al [47] suggest that cupper oxalate incorporates little or no water of crystallization in the crystal lattice. Kinetics of the thermal decomposition of cupper oxalate in N_2 was reported by Coetzee et. al. [48].

Thermal decomposition of $FeC_2O_4.2H_2O$ was investigated in air, oxygen and inert atmosphere, using DTA-TG, Mössbauer spectroscopy and X-ray phase analysis [49]. Conflicting results have been published on the decomposition. TG studies in air by Robin and Bernard [50] indicated that dehydration commenced in the region of 423°K and was closely followed by decomposition at 473°K. Dollimore et. al. [17] failed to observe a dehydration plateau during TG studies in air and N_2, but Boulle and Doremieux [51] found that water was removed at about 403-413°K followed by a decomposition at a temperature which varied with the nature of ambient atmosphere. Nicholson [52] showed that the decomposition of FeC_2O_4 followed dehydration, when studying the decomposition of very small sample (3mg) in O_2 and obtained inflection

in TG curve, corresponds to anhydrous oxalate formation. Broadbent et. al. [53] showed that it is possible under N_2 atmosphere to prepare anhydrous ferrous oxalate by heating at 473°K and showed that the endo peak of dehydration in air can be seen but it is swamped by the large exo decomposition peak. The X-ray analysis shows that the final decomposition product in air is Fe_2O_3 and in N_2 the residue heated at 903°K was found to be free iron, Fe_3O_4 and trace of FeO. Coetzee et. al.[48] reported the thermal decomposition of ferrous oxalate in air and N_2 and founded that the residue after decomposition in N_2 to be FeO and in O_2 to be Fe_2O_3. The isothermal decomposition kinetic of ferrous oxalate in N_2 is mainly declaratory (R_3). The kinetic studies considering both isothermal and non-isothermal techniques for thermal decomposition of ferrous oxalate were also reported [54].

Dollimore and Griffith [18] reported the DTA curves for cobalt oxalate in N_2 and air. Dollimore et. al. [17] showed that the end product in air to be Co_3O_4, but in N_2 it is Co metal. Macklen [27] showed that, the endothermic dehydration is quickly followed by a strongly exothermic decomposition, which shows up as a sharp peak in the DTA curves over the temperature range 526-573°K. Coetzee et. al. [48] reported that the decomposition in N_2 started at about 613°K and complete at 703°K with formation of Co residue, whereas in oxygen the onset is about 553°K and the residue is closest to Co_3O_4 and the reaction is strongly exothermic. The kinetics of the thermal dehydration of $CoC_2O_4.2H_2O$ were reported by Mu and Perlmutter [55] where it is found that the

dehydration obeys the first order model (F_1) with activation energy of 158±1 kJ/mol.

$NiC_2O_4.2H_2O$ is a green powder, which when heated to 423-453°K in vacuo, loses two moles of water of crystallization to yield the dehydrated form, which is a high yellow powder takes up water from the atmosphere during handling [40]. TG analysis of $NiC_2O_4.2H_2O$ shows that the final product in air is nickel oxide and that in nitrogen it is nickel [17]. In the decomposition of $NiC_2O_4.2H_2O$ [56] a change from endo decomposition peak in N_2 to an exo peak in O_2 is observed, because the metal produced is oxidized. Various workers [27,40,55,56] have reported the thermal decomposition of nickel oxalate.

TG analysis of $MnC_2O_4.2H_2O$ shows that the final product in air is Mn_2O_3 and that in N_2 it is MnO. A number of the publications deal with the kinetics of $MnC_2O_4.2H_2O$ decomposition were reported [27,57].

The double oxides of Li and Cu was first prepared by Troost [58] who described it as a compound forms sky-blue needles, has a formula; LiC_2O_4, CuC_2O_4, $2H_2O$. Mixed metal oxalates have been used as precursors for the preparation of important materials such as $BaTiO_3$ [59]. Schuele [60] prepared ferromagnetic and ferrimagnetic fine particles (of mixed oxides) by suitable heat treating of co-precipitated oxalates of Co-Fe, Ni-Fe and Cu-Fe systems in a wide range of compositions. Robin [23] indicated that some of bimetal oxalates form solid solution by decomposing thermally at moderate temperatures and yielding metal oxides and easily removed gaseous products. Co-precipitated mixture of

silver and mercurous oxalates containing 50-60 mole percent of the latter exhibit very much higher rates of photo thermal decomposition than do the separate compounds. X-ray diffraction studies showed no evidence of new compound or solid solution formation. The material is the basis for photothermography [61]. Preparation and thermal analysis of mixed Mg-Mn-iron oxalates have been studied by Gallagher and Schrey [62]. The thermal decomposition of mixed cerium-gadolinium oxalates containing 20 and 50 mol% gadolinium were studied [63]. The thermal behaviour of the mixed metal oxalates [64]; $FeCu(OX)_2.3H_2O$, $CoCu(OX)_2.3H_2O$ and $NiCu(OX)_2.3.5H_2O$ [where $OX=C_2O_4$] prepared by co-precipitation from solutions has been examined using thermogravimetric analysis in air and nitrogen atmospheres. The thermal behaviour of the mixed oxalate, $MCu(OX)_2.xH_2O$ [M= Fe, Co and Ni], differed from that of the individual metal oxalates.

Both isothermal and programmed temperature experiments [48] have been used to obtain kinetic parameters for the dehydrations and decompositions in nitrogen of the mixed metal oxalates; $MCu(OX)_2xH_2O$. Results are compared with those reported for the thermal decomposition of the individual metal oxalates.

Metal oxalates are considered, as a clean route for production of metal or metal oxides when thermally decomposed at moderately low temperatures, therefore mixed metal oxalates were used to produce mixed metal oxides after; their decomposition. Mixed oxides of Fe_2O_3-NiO [65], Fe_2O_3-Cr_2O_3 [66] were prepared by co-precipitation of

$Fe(OH)_3/Ni(OH)_3$ and the thermal treatment of hydroxide co-precipitates up to 1073 or 1373°K. Mixed oxides of $CuO\text{-}Cr_2O_3$ [67] can be prepared by calcination of co-precipitated carbonates in air.

Fujita et. al. [26] studied infrared spectra of most metal oxalates, since its structure is simple and assignment of different bonds is available. Douville et. al. [68] measured the infrared spectra of most oxalates, but they didn't give any discussion on the relation between the stability and band shift. Ristic et. al. [69] proved that, vibrational spectroscopy is a very useful technique for detection of chemical and structural changes in mixed metal oxides. The degree of crystallinity strongly affects the infrared spectra of hematite. FT-IR spectroscopy was used to follow the changes in chemical and structural properties of mixed metal oxides of $Fe_2O_3\text{-}NiO$ [65], $Fe_2O_3\text{-}Cr_2O_3$ [66], $CuO\text{-}Cr_2O_3$ [67] and $Fe_2O_3\text{-}In_2O_3$ [69].

The X-ray diffraction of most oxalate salts were studied by Dusansay et. al. [70]. Lagier et. al. [71] studied the structure of $MC_2O_4.2H_2O$ using x-ray analysis and concluded that the structure is as follow:

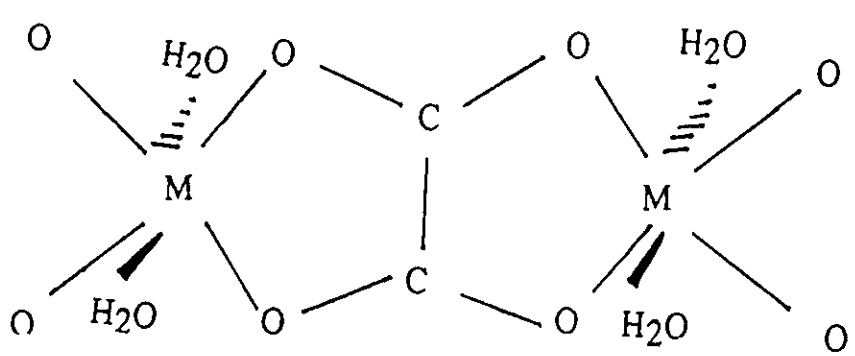

where the oxalate ions act as a quadridentate ligand and the water molecules were coordinated directly to the metal ions.

The oxide phases were identified using the data contained in the powder diffraction file. X-ray diffraction technique was used to identify chemical and structural changes in mixed metal oxides of Fe_2O_3-NiO [65], Fe_2O_3-Cr_2O_3 [66], CuO-Cr_2O_3 [67] and Fe_2O_3-In_2O_3 [69].

In the literature [72] it was found that ZnO has wurtzite structure; Fig.(I-1) in which each Zn^{2+} is joined to four O^{2-} ions in a system of puckered hexagons. While CdO has the normal sodium chloride structure. But NiO has full cubic symmetry only at higher temperatures, and becomes less symmetrical (rhombohedral) at lower temperatures. Also it was found that CuO has PtS structure [72]; Fig.(I-1) which formed from, nets with planer and tetrahedral coordination. It consists from Cu^{2+} ions form for coplanar and O^{2-} ions form for tetrahedral bonds. For Co_3O_4, the crystal has the spinel structure; Fig.(I-1) which is like sodium chloride structure. It may be described in terms of oxide ions in a close-backed cubic arrangement. One half of the octahedral cavities (B-sites) and one-eighth of the tetrahedral cavities (A-sites) are occupied by cations having requisite valence to neutralize the charge of the oxide ions. The unit cell formula is $A_8B_{16}O_{32}$ where A and B represent the different cation sides i.e. Co_3O_4 structure may be written as:

$$[Co_8^{2+}]_t[Co_{16}^{3+}]_oO_{32}$$

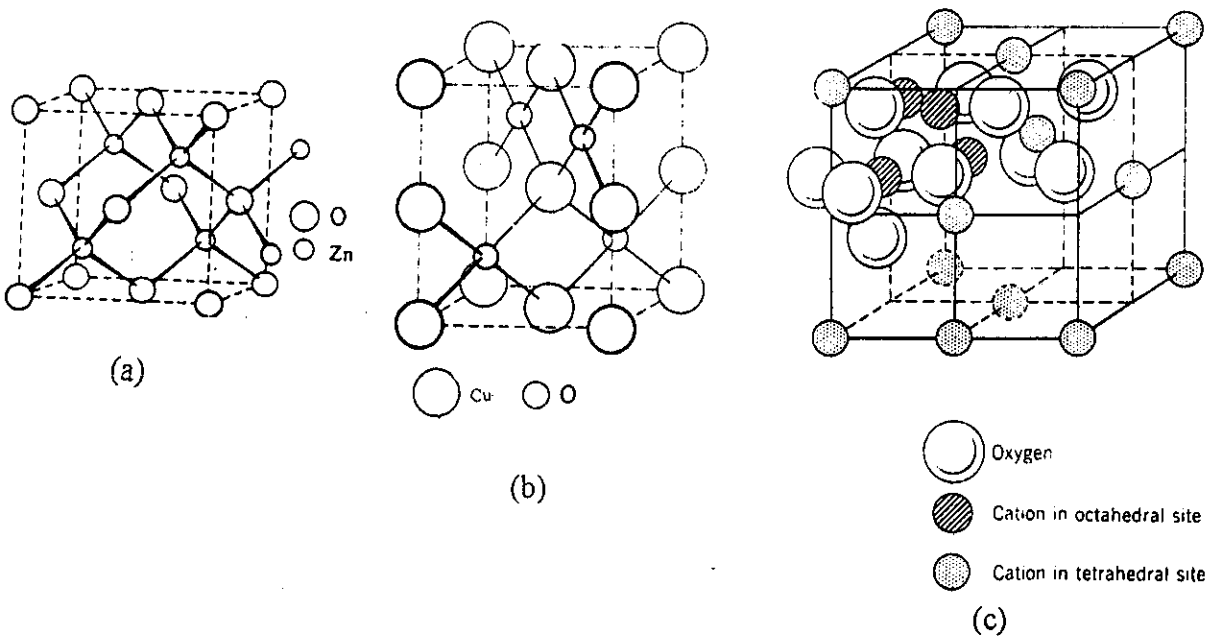

Fig.(I-1): The structure of (a) ZnO, (b) CuO and (c) Co_3O_4.

Fe_2O_3 has polymerphic structures α and γ [72]. The α structure (corundum structure) is an approximately hexagonal closed pack array of O^{2-} ions in which Fe^{3+} ions occupy two-thirds of the octahedral holes. The structure is complex, for there is sharing of vertices, edges and faces of FeO_6 coordination groups. There are two sets of Fe-3O, 1.945 Å and Fe-3O, 2.116 Å. The structure of the second (γ) form of Fe_2O_3 is related in an interesting way to the structure of NaCl and inverse spinel. In γ-Fe_2O_3 there are on the average only $21\frac{1}{3}$ Fe^{3+} ions per unit cell distributed at random among the eight tetrahedral and sixteen octahedral sites. For Mn_2O_3 there are two forms of structure α and γ. α having the C sesquioxide structure and γ shows the type of tetragonal distortion [72].

The electrical properties of materials depend on whether the materials are conductors or insulators and, if the former, on whether the current carriers are electrons or ions. Electrical conductivity occurs to varying extent by different mechanism in a wide variety of materials. It is responsible for the characteristic electrical properties of metals, superconductors and semiconductors [11]. The electrical conductivity of transition metal oxides are much less fully understood than those of the classical semiconductors based on silicon and germanium. Oxides of the transition metals nearly always display effects due to mixed valences because a change of stoichiometry can be accommodated by a change in the occupation number of d-shell. Two classes of metal oxides can be distinguished, the saturated oxides, in which all of d-electrons of transition metal atoms have been given off to oxygen atoms, and the unsaturated oxides, in which there is an unfilled shell of electrons remaining on some of transition metal ions after they reach their appropriate valence state. Several transition metal oxides are semiconducting at low temperatures but at given temperature or over a small temperature range their conductivity suddenly jumps by a large factor, as great as 10^7, and at higher temperature the materials are metallic [73]. Electronic conductivity as a function of temperature for several unsaturated binary transition metal oxides were reported by Alder [74]. The electronic properties of transition metal oxide gels arise from electron transfer between transition metal in different oxidation states [15]. Recently mixed metal oxides having the general formula

XY_2O_4 [75,76] have been investigated as they exhibit interesting structure, electrical, magnetic and catalytic properties. Classes containing transition metal oxides are a subject of contineous interest because of the possible application due to their semiconducting properties. It is well known that the electron conductivity in this kind of glasses is due to a thermally activated hopping process of d-electrons between ions in different valence states[74]. Mousa et. al. [76] reported that the hopping mechanism between Co^{2+} and Co^{3+} ions is the predominate conduction mechanism in ferrites containing higher concentration of cobalt. Mousa et. al. [75] reported that the conductivity of $Zn_X Fe_{3-X}O_4$ spinel for $0 \leq x \leq 0.79$ can be interpreted as due to an electron exchange between Fe^{2+}/Fe^{3+} ions laying on octahedral sites (hopping mechanism), whereas for $x > 0.79$ the conduction may proceed through cation vacancies. Mousa [78] reported that the electrical conductivity of Cu- doped Fe_3O_4 occurred by a hopping mechanism due to fast electron exchange between Fe^{2+} and Fe^{3+} present on octahedral sites.

Cadmium oxide [79] is a typical n-type semiconductor. Zinc oxide [80] is also n-type semiconductor with band gap energy of about 3.2ev at room temperature. Bonasewicz et. al. [81] investigated the conductivity of pure zinc oxide films in temperature range 300 to 1000°K in oxygen. Zuev [82] and Kapp et. al. [83] studied the conductivity of CuO. It has been reported that α-Fe_2O_3 [84] is a semiconductor in the temperature range 293-1623°K. Co_3O_4 [85] has a normal spinel structure where the conductance occurs via electron exchange takes place between Co^{2+} and

Co^{3+} ions on equivalent lattice sites. NiO [86] is a p-type semiconductors, and conductivity always increase exponentially with temperature.

Transition metal oxides show different magnetic properties, which depends to a large extent on their electronic structures. The oxides of early elements; TiO, VO and CrO are diamagnetic [11]. The oxides of the latter elements; MnO, FeO, CoO and NiO are paramagnetic at high temperature and exhibit ordered magnetic structures at low temperatures. These oxides are all antiferromagnetic at low temperature and change to paramagnetic above the Neel temperature; T_N. and all have similar structures in both the antiferromagnetic and paramagnetic forms. Materials that are competing for applications as permanent magnets are likely to be based on the metal Fe, Co, Ni [11]. Ferromagnetic and ferrimagnetic fine particles [60] were prepared by suitable heat treatment of co-precipitated oxalates of Ni-Fe and Cu-Fe systems in a wide range of compositions.

I-3. Aim of the Work:

Recently, electrical and magnetic properties of solids containing mixed valency states and cations having different oxidation states attract the attention of many investigators, because of their great and promising application, as electronic devices. The present study was carried out to throw more light on the structural, thermal, magnetic and electronic properties of some metal oxalates and oxides having mixed valency state ions as well as to study the effect of adding impurities such as silver

Theories and Methods of Calculation

II-1. Kinetic Analysis of Non-Isothermal TG Data:

With dynamic technique, the temperature of the system is usually set to increase at a constant rate; β, and the function g(α) is given by Doyle's equation[87]:

$$g(\alpha) = (A/B)\int_0^T \exp(-E/RT)dT = \frac{AE}{R\beta}P(x) \qquad (1)$$

where g(α) depends on the mechanism controlling the reaction and on the size and shape of the reacting particle. The function P(*x*) has been defined as:

$$P(x) = \frac{e^{-X}}{x}\int_x^{\infty}\frac{e^{-u}du}{u} \qquad (2)$$

where u=E/RTand *x* is the corresponding value of u at which a fraction α of the material has decomposed.

In Coats-Redfern method [88], the function g(α) is approximated to the form:

$$g(\alpha) = \frac{ART^2}{\beta E}\left[1-\frac{2RT}{E}\right]e^{-E/RT} \qquad (3)$$

where α is the fraction of sample decomposed at time t and β is the heating rate.

The equation has been written in the form:

$$-\ln[g(\alpha)/T^2] = -\ln\frac{AR}{\beta E}\left(1-\frac{2RT}{E}\right)+\frac{E}{RT} \qquad (4)$$

The quantity ln[AR/βE(1-2RT/E)] appears to be reasonably constant for most values of E and in the temperature range over which most reaction occur. The correct form of g(α) must be used in equation (4) in order to allow the calculation of activation energy. A plot of

$-\ln[g(\alpha)/T^2]$ versus 1/T should result in a straight line of slope (E/R) from which the activation energy (E) can be calculated. Another approximate integral method which is recently used to obtain kinetic parameters from dynamic TG curves is that proposed by Ozawa[89]. A master curve has been derived from the TG data obtained at different heating rates (β) using Doyle's equation [87] and assuming that [(AE/Rβ)P(E/RT)] is a constant for a given fraction of material decomposed. The function P(E/RT) was approximated by the equation:

$$\log P(E/RT) = -2.315 - 0.4567(E/RT) \qquad (5)$$

so that,

$$-\log \beta = 0.4567(E/RT) + \text{constant} \qquad (6)$$

hence the activation energy may be obtained from the TG data obtained at different heating rates, by the plot of log β versus 1/T for different α-values. The frequency factor; A was calculated from equation:

$$\log A = \log g(\alpha) - \log\left[\frac{E}{\beta R} P(E/RT)\right] \qquad (7)$$

The calculation of E is independent of the reaction model used to describe the reaction, whereas the frequency factor depends on the determined form of $g(\alpha)$.

In the composite methods of analysis of dynamic data [90], the results obtained not only at different heating rates but also with different values of α, are superimposed on one master curve. In the application of composite method (I), use has been made of the modified Coats-Readfern equation [91]:

$$\frac{g(\alpha)}{T^2} = \frac{AR}{\beta E} e^{-(E/RT)} \tag{8}$$

the equation was rewritten in the form:

$$\ln[\beta\, g(\alpha)/T^2] = \ln (AR/E) - (E/RT) \tag{9}$$

Therefore, the dependence of $\ln[\beta(g(\alpha)/T^2)]$, calculated for different α-values at their respective β values, on 1/T must give rise to a single master straight line for the correct form of $g(\alpha)$, and hence a single activation energy and frequency factor can readily be calculated. The second approach for composite analysis of data depends on Doyle's equation:

$$g(\alpha) = AE/R\beta\, P(E/RT) \tag{10}$$

again, using the approximation given above for the function P(E/RT), this equation may be rewritten as:

$$\log g(\alpha)\, \beta = [\log AE/R - 2.315] - 0.4567\, E/RT \tag{11}$$

hence, the plot of the left side of this equation, for different values of α at their respective β values versus 1/T must give rise to a single master straight line, from the slope and intercept of which single values for both E and logA may be calculated. The composite approach involves a complete analysis of all non-isothermal curves into a single curve. The kinetic analysis of non-isothermal data was performed with reference to the different models of heterogeneous solid-state reactions, based on the composite method of analysis, then the model which will give best fit to the experimental data will be used to calculate kinetic parameters, assuming different methods previously discussed.

Tab.(II-1) lists some of the more important kinetic equations given in the literature [8,90-96] which we have examined to find the most appropriate kinetic expression and reaction model which describes the reaction under various conditions.

In the diffusion controlled reaction, the reaction rate is governed by diffusion, e.g. of a gaseous product through a continuos product layer; D_1 is for one dimensional diffusion process governed by a parabolic law, with constant diffusion coefficient; D_2 is a two dimensional diffusion-controlled process into a cylinder, D_3 is Jander's equation for a diffusion controlled reaction in a sphere, D_4 is the Ginstling-Braunshtein equation for a diffusion controlled reaction starting on the exterior of a spherical particle and D_5 the Zhuravlev-Lasokhim-Tenpel'man diffusion equation. If the reaction is controlled by movement of an interface at constant velocity and nucleation occurs virtually instantaneously, then for such phase boundary controlled reaction equation relating α and t are the R_2 function (contracting area) for a circular disc reacting from the edge inward, and the contracting sphere or R_3 model for a sphere reacting from the surface inward. If the solid-state reaction is controlled by nucleation followed by growth, then in this case we may have Mampel unimolecular law, in which the rate determining step is the nucleation process described by F_1 function or first order kinetics. Function F_2 and F_3 are given, for second and third order kinetic respectively. In phase boundary reactions, it is assumed that the nucleation step occurs instantaneously, so that the surface of each particle s covered with a

Tab.(II-1): Kinetic model equations used in this work

Reaction model	Symbol	g(α)	f(α)
Two dimensional phase boundary	R_2	$1-(1-\alpha)^{1/2}$	$2(1-\alpha)^{1/2}$
Three dimensional phase boundary	R_3	$1-(1-\alpha)^{1/3}$	$3(1-\alpha)^{2/3}$
One dimensional diffusion	D_1	α^2	$1/2\ \alpha$
Tow dimensional diffusion	D_2	$\alpha+(1-\alpha)\ln(1-\alpha)$	$-1/\ln(1-\alpha)$
Three dimensional diffusion	D_3	$[1-(1-\alpha)^{1/3}]^2$	$3(1-\alpha)^{2/3}/2[1-(1-\alpha)^{1/3}$
Four dimensional diffusion	D_4	$(1-2/3\alpha)-(1-\alpha)^{2/3}$	$3/2[(1-\alpha)^{-1/3}-1]$
Random nucleation	A_2	$[-\ln(1-\alpha)]^{1/2}$	$2(1-\alpha)[-\ln(1-\alpha)]^{1/2}$
Random nucleation	A_3	$[-\ln(1-\alpha)]^{1/3}$	$3(1-\alpha)[-\ln(1-\alpha)]^{2/3}$
Random nucleation	A_4	$[-\ln(1-\alpha)]^{1/4}$	$4(1-\alpha)[-\ln(1-\alpha)]^{3/4}$
First order kinetics	F_1	$-\ln(1-\alpha)$	$(1-\alpha)$
Second order kinetics	F_2	$1/(1-\alpha)$	$(1-\alpha)^2$
Third order kinetics	F_3	$[1/(1-\alpha)]^2$	$(1-\alpha)^3$
Prout-Tompkins	B_1	$\ln[\alpha/(1-\alpha)]$	$\alpha(1-\alpha)$
Exponential law	E_1	$\ln\alpha$	α

layer of product nucleation of the reactants, however may be a random process, not followed by rapid surface growth. As nuclei grow larger they may eventually impinge on one another, so that growth ceases where they touch. Avrami and Erofeev, who have given the functions A_2, A_3 and A_4, have considered this process. For branching nuclei, Prout-Tompkins [90] gave the function B_1. The E_1 function is for the exponential law.

II-2. Electrical conductivity:

Determining transport properties is one of the most informative macroscopic measurements that can be performed on solid materials, and the information obtained can be related both to the nature of the bonding and the dynamical properties of the lattice. However, as with all macroscopic measurements, the results do not directly lead to microscopic parameters; instead transport data may suggest a model of the electronic structure. The prediction of this model may then be checked by spectroscopic, magnetic and thermal data, and by reference to the crystal structure.

The electrical conductivity measurement is one of the most important methods, which can be used to give information on the transport of charge carriers in the solids. The electrical conductivity "σ" of any material is given by the product of the number of charge carriers "n" and their mobility μ`. [11]

$$\sigma = n\, e\, \mu` \qquad (12)$$

where e is the charge of the carrier.

The materials can be classified into different types depending on their conductivity values: metal, semiconductors, insulators and superconductors. The electrical conductivity for any particular metal is being caused by imperfections in the metal lattice. In semiconductors and insulators the situation is quite different. Unlike that for metals, the number of conducting electrons varies with temperature and field, giving rise to the conductivities whose dependence on temperature and field is quiet specific.

The electronic structure of semiconductors and insulators [11] produced from the overlap between orbitals of neighbouring atoms or ions to give rise to a series of narrowly spaced energy levels termed bands. The highest occupied band is called the valence band (VB) and the lowest unoccupied band, the conduction band (CB); Fig.(II-1). In between the CB and VB is an energy gap called the bandgap.

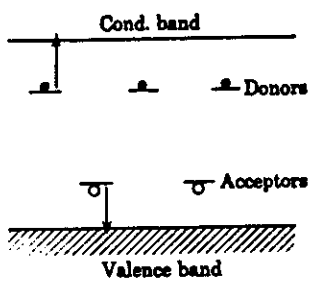

Fig(II-1): Energy levels in an insulator or semiconductor.

Excitation of the electron from the VB leaves behind a vacancy or "hole". Electrons in the VB can move to fill these holes leaving, in turn further holes. Consequently, it is easier to consider the holes moving in a sea of immobile electrons. Introducing impurities into semiconductors or insulators cause a change in concentration of electrons and/or holes. These impurities may be neutral or ionize, releasing electrons into the conduction band, or they may capture electrons, releasing holes into the VB. The former type of impurity leads to an "n-type" semiconductor, the latter to a "p-type" material

The temperature dependence of conductivity is usually given by the Arrhenius equation:

$$\sigma = \sigma_0 \exp(-E_a/kT) \qquad (13)$$

where E_a is the activation energy required for migration of charge carriers, k is the Boltzmann constant and T is the absolute temperature. The pre-exponential factor; σ_0, contains several constants, including the vibrational frequency of the potentially mobile charge carriers. Graphs of $\ln\sigma$ against 1/T should give straight lines of slope $(-E_a/k)$ from which one can calculate the value of activation energy.

The density of charge carriers is given by equation:

$$n = 2\left(\frac{2\pi mkT}{h^2}\right)^{3/2} \exp(-E_a / kT) \qquad (14)$$

where m* is the effective mass of charge carriers (assumed to be equal to the rest mass of electron), h is the Blanck's constant and E_a is the activation energy. This equation is approximated as:

$$X_M = X_g .molecular\text{-}\ weight = \frac{2m\lg}{M(H_0^2 - H_1^2)} \times molecular\text{-}\ weight \qquad (20)$$

and it has units of e.m.u./mole. For normal paramagnetic and dimagnetic substances X_M is constant independent of field strength.

When substance has an unusually large X_M, it is referred to as a ferrimagnetic material. Ferromagnetism results when magnetic dipoles in a substance can interact with one another causing extensive alignment of the moments with the field; very large values of "I" result. For these materials the susceptibility is field-strength dependent.

The susceptibility of different kinds of magnetic material are distinguished by their different temperature dependence. Many paramagnetic substances obey the simple curie law, especially at high temperature [98]. This states that the magnetic susceptibility is inversely proportional to temperature:

$$X_M = C/T \qquad (21)$$

Where C is the Curie constant. Often, however, the Curie-Weiss law provides a better fit to the experimental data: [98]

$$X_M = C/(T+\theta) \qquad (22)$$

where θ is an empirical constant called the Weiss constant. The deviation from the Curie law is due to interionic or intermolecular interactions. As a result of these interactions the orientations of the magnetic dipoles are influenced by the orientations of the neighbours.

The Curie constant can be obtained by plotting X^{-1}_M versus T, where straight line with slope = C is obtained.

The deviation from the Curie-Weiss law can also be observed by plotting $X_M T$ versus T.

For all materials, the effect of increasing temperature is to increase the thermal energy possessed by ions and electrons. There is therefore, a natural tendency for increasing structural disorder with increasing temperature. For paramagnetic materials, the thermal energy of ions and electrons acts to partially cancel the ordering effect of the applied magnetic field. Thus, X_M decreases with increasing temperature in Curie/Curie-Weiss law fashion [11].

For ferro and antiferromagnetic materials, the effect of temperature is to introduce disorder into the otherwise perfectly ordered parallel/antiparallel arrangement of spins. For ferromagnetic materials, this leads to a rapid decrease in X with increasing temperature. For antiferromagnetic materials, this leads to decrease in the degree of antiparallel ordering, an increase in the number of disorder electron spins and hence an increase in X [11].

The magnetic properties of materials are often expressed in terms of the magnetic moment; μ, since this is a parameter that may be related directly to the number of unpaired electrons present. The relationship between X_M and μ is:

$$X_M = \frac{N\beta^2\mu^2}{3KT} \tag{23}$$

where N is Avagadro's number, β is the Bohr magneton and k is Boltzmann's constant. Substituting for N, β and k givses:

$$\mu_{eff} = 2.83\sqrt{X_M T} = 2.83\sqrt{C} \tag{24}$$

this equation holds for substances that obey the Curie-Weiss law: X_M = C/T. While for the substances obey the Curie-Weiss law, μ should be calculated from the susceptibility by equation:

$$\mu_{eff} = 2.38\sqrt{X_M(T+\theta)} = 2.83\sqrt{C} \quad (25)$$